

**SYNTHESIS, CHARACTERIZATION AND
CATALYTIC STUDIES OF NANOCRYSTALLINE
Cs-ABW ZEOLITE IN HENRY REACTION OF
BENZALDEHYDE AND NITROALKANES**

TAMARA MAHMOUD ALI GHREAR

UNIVERSITI SAINS MALAYSIA

2020

**SYNTHESIS, CHARACTERIZATION AND
CATALYTIC STUDIES OF NANOCRYSTALLINE
Cs-ABW ZEOLITE IN HENRY REACTION OF
BENZALDEHYDE AND NITROALKANES**

by

TAMARA MAHMOUD ALI GHREAR

**Thesis submitted in fulfilment of the requirement
for the degree of
Doctor of Philosophy**

February 2020

ACKNOWLEDGEMENT

Thank and praise to Allah, who has helped me in completing this work. I would like to express my deepest appreciation and sincere gratitude to my supervisor, Assoc. Prof. Dr. Ng Eng Poh, and my co-supervisor, Assoc. Prof. Dr. Tan Soon Huat for their guidance, assistance, immense contribution, valuable suggestions and encouragement towards completing this project. I also would like to acknowledge School of Chemical Sciences, Universiti Sains Malaysia and Université de Caen for the needed facilities and instruments. I would like to extend my appreciation to FRGS (203/PKIMIA/6711642) and RUI (1001/PKIMIA/8011012) grants for the financial support. Special thanks also go to all academic and non-academic staff of School of Chemical Sciences, USM that have contributed enormously throughout my research. Finally, great gratitude also goes to my labmates and my family especially my husband Kamal for his concern, encouragement and help when I felt upset during my PhD journey.

TABLE OF CONTENTS

ACKNOWLEDGEMENT	ii
TABLE OF CONTENTS	iii
LIST OF TABLES	vii
LIST OF FIGURES	viii
LIST OF ABBREVIATIONS, NOMENCLATURES AND SYMBOLS	xiii
ABSTRAK	xv
ABSTRACT	xvii
CHAPTER ONE INTRODUCTION	1
1.1 General introduction	1
1.2 Research objectives	5
1.3 Overview of the thesis	5
CHAPTER TWO LITERATURE REVIEW	8
2.1 Introduction of zeolites	8
2.2 Zeolite structures and properties	11
2.3 Nomenclature of zeolites	12
2.4 Formation of zeolites	13
2.5 Synthesis of zeolites	15
2.6 Effect of synthesis parameters on the formation of zeolites	17
2.6.1 Sources of silica and alumina	18
2.6.2 Effect of the Si/Al ratio	19
2.6.3 Alkalinity	20
2.6.4 Effect of temperature	21
2.6.5 Effect of time	22
2.6.6 Effect of mineralizing agents (OH ⁻ and F ⁻)	23
2.6.7 Effects of water content	24
2.6.8 Effect of organic template	25

2.6.9	Effects of zeolite seeds	27
2.7	Nanozeolites.....	28
2.8	ABW-type zeolite	32
2.9	Disposal and recycling of mother liquor.....	35
2.10	The origin of acidity and basicity of zeolites.....	35
2.11	Henry (nitroaldol) reaction of benzaldehyde and nitroalkanes	37
2.12	Modes of heating.....	38
2.12.1	Microwave heating	38
2.12.2	Non-microwave instant heating.....	39
CHAPTER THREE MATERIALS AND EXPERIMENTAL METHODS		41
3.1	Introduction.....	41
3.2	Chemicals.....	41
3.3	Time dependent and other synthesis parameters studies of the formation of nanosized Cs-ABW.....	42
3.4.	Microwave-assisted hydrothermal synthesis of nanosized Cs-ABW	45
3.5	Recyclable synthesis of Cs-ABW zeolite nanocrystals	46
3.6.	Characterization techniques	47
3.6.1	X-ray powder diffraction (XRD) analysis	48
3.6.2	Fourier transform infrared (FTIR) spectroscopy	49
3.6.3	Transmission electron microscopy (TEM).....	50
3.6.4	Solid-state magic-angle spinning nuclear magnetic resonance spectroscopy (MAS NMR).....	51
3.6.5	Field emission scanning electron microscopy (FESEM)	53
3.6.6	Energy dispersive X-ray (EDX) spectroscopy	53
3.6.7	Inductively coupled plasma optical emission spectrometry (ICP-OES)	54
3.6.8	Nitrogen (N ₂) gas adsorption-desorption analysis.....	54

3.6.9	Thermogravimetry/Differential thermogravimetry (TGA/DTG) analysis	56
3.6.10	Temperature-programmed desorption of carbon dioxide (TPD-CO ₂).....	56
3.6.11	Gas chromatography (GC) analysis.....	57
3.6.12	Mass spectrometry (MS)	58
3.7	Catalytic nitroaldol reaction of benzaldehydes with nitroalkanes	59
CHAPTER FOUR SYNTHESIS OF Cs-ABW NANOZEOLITE IN ORGANOTEMPLATE-FREE SYSTEM.....		61
4.1	Introduction.....	61
4.2	Results and discussion	62
4.2.1	Effect of synthesis parameters on the formation of ABW nanosized zeolite	62
4.2.1(a)	Effect of Cs ₂ O content	62
4.2.1(b)	Effect of H ₂ O content.....	63
4.2.1(c)	Effect of SiO ₂ content	64
4.2.1(d)	Effect of metal hydroxide	65
4.2.1(e)	Effect of synthesis temperature.....	66
4.2.2	Time dependent study of the formation and crystal growth of Cs-ABW nanocrystals.....	67
4.2.3	Formation of Cs-ABW nanocrystals under microwave heating environment	77
4.3	Summary	87
CHAPTER FIVE ORGANOTEMPLATE-FREE Cs-ABW NANOZEOLITE AS HIGHLY REACTIVE AND RECYCLABLE CATALYST FOR HENRY REACTION BETWEEN BENZALDEHYDES AND NITROETHANES.....		89
5.1	Introduction.....	89
5.2	Results and discussion	89
5.2.1	Synthesis of Cs-ABW zeolite nanocrystals.....	89
5.3	Catalytic Henry reaction between benzaldehyde and nitroethane	94

5.3.1	Effect of reaction temperature and time	95
5.3.2	Effect of catalyst loading.....	97
5.3.3	Effect of benzaldehyde to nitroethane molar ratio	98
5.3.4	Effects of solvent.....	99
5.3.5	Catalyst comparative study.....	101
5.3.6	Effect of reaction mode	103
5.3.7	Nitroaldol reaction between benzaldehyde derivatives with nitroalkanes.....	104
5.3.8	Catalyst reusability test.....	105
5.4	Reaction mechanism	108
5.5	Summary	109
CHAPTER SIX	RECYCLABLE SYNTHESIS OF Cs-ABW ZEOLITE NANOCRYSTALS FROM NON- REACTED MOTHER LIQUORS WITH EXCELLENT CATALYTIC HENRY REACTION PERFORMANCE	110
6.1	Introduction.....	110
6.2	Results and discussion	111
6.3	Summary	123
CHAPTER SEVEN	CONCLUSIONS AND FUTURE WORKS.....	124
7.1	Conclusions.....	124
7.2	Recommendation of future works.....	125
REFERENCES.....		127
APPENDICES		
LIST OF PUBLICATIONS		

LIST OF TABLES

	Page
Table 2.1	Some examples of structure types. 13
Table 2.2	Nanosized zeolites and their synthesis conditions..... 34
Table 3.1	Synthesis conditions of Cs-ABW nanozeolite. 44
Table 3.2	Possible vibration bands in the fingerprint region of zeolite frameworks. 50
Table 3.3	GC-FID oven-programmed setup for studying catalytic Henry reaction. 58
Table 3.4	GC-MS oven-programmed setup for studying catalytic Henry reaction. 59
Table 4.1	Chemical elemental analysis of the solid products obtained after various heating times..... 75
Table 4.3	Selected bond distances (Å) in Cs-ABW zeolite nanocrystals. 81
Table 4.4	Crystallographic data of Cs-ABW zeolites. 82
Table 4.5	ICP-OES spectroscopy data of MW-6m. 85
Table 5.1	EDX chemical analysis of HT-60m (zeolite Cs-ABW). 93
Table 5.2	Effect of solvent on nitroaldol condensation reaction. 100
Table 5.3	Comparison of nanosized Cs-ABW zeolite catalyst with reported homogenous catalyst systems. 102
Table 5.4	Conversion of benzaldehyde with Cs-ABW nanocatalyst under different heating methods..... 104
Table 5.5	Catalytic nitroaldol reaction of benzaldehyde derivatives with nitroalkane. 105
Table 6.1	Reacting precursor suspensions and crystalline yield of Cs-ABW nanocrystals. 112
Table 6.2	Chemical compositions and textural properties of Cs-ABW zeolite nanocrystals. 118
Table 6.3	Catalytic nitroaldol condensation of benzaldehyde with nitroethane under microwave irradiation..... 122

LIST OF FIGURES

		Page
Figure 2.1	The basic structure of zeolites with n repeating units where negative charge of Al site is charge balanced by metal cations (M ⁺).....	8
Figure 2.2	Ring size of zeolites.....	10
Figure 2.3	Some examples of zeolites with different pore sizes and pore dimensions.....	10
Figure 2.4	(a) Primary building units (PBUs): (SiO ₄) ⁴⁻ or (AlO ₄) ⁵⁻ , (b) secondary building units (SBUs), (c) composite building units (CBUs), and (d) structures of zeolites.....	12
Figure 2.5	The kinetics of (a) nucleation and (b) crystal growth of zeolites, and (c) the mechanism of the conversion of amorphous particles into crystalline zeolite framework.....	15
Figure 2.6	Processes of zeolite synthesis: (a) selection of initial chemical reagents, (b) preparation of precursor mixture (dense gel or colloidal suspension), (c) crystallization of zeolites, (d) purification, and (e) calcination of as-synthesized zeolite crystals.....	17
Figure 2.7	Crystallization kinetics of zeolite A influenced by the alkalinity of the precursor hydrogel of 5Na ₂ O:Al ₂ O ₃ :2SiO ₂ :100–200H ₂ O at 70 °C.....	21
Figure 2.8	Phase transformation of Na-zeolites under increasing hydrothermal heating time and/or temperature.	22
Figure 2.9	Statistical publication data on the number of zeolite frameworks synthesized at various water contents (molar ratios of 10 OH: z H ₂ O).....	25
Figure 2.10	Several zeolite frameworks synthesized using organic cations with different sizes and shapes.....	27
Figure 2.11	The methods that have been used for the synthesis of nanozeolites.	29
Figure 2.12	Example of the synthesis of ZSM-5 nanozeolite using space confinement method where L ₁ and L ₂ are the diameters of ZSM-5 crystal and mesopore opening of the inert matrix, respectively).....	30
Figure 2.13	ABW zeolite structure	33

Figure 2.14	(a) Brönsted basic and (b) Brönsted acid sites of zeolites.....	36
Figure 2.15	Microwave dielectric heating via (a) migration of ionic atoms/molecules and (b) rotation of dipolar atoms/molecules (Kappe, 2004).....	39
Figure 2.16	Non-microwave instant heating reactor (Obermayer et al., 2016).....	40
Figure 3.1	The flow of synthesis process of nanosized Cs-ABW zeolite.	45
Figure 3.2	The synthesis process of nanosized Cs-ABW via microwave-assisted hydrothermal condition.....	46
Figure 3.3	The procedure of recyclable synthesis of Cs-ABW zeolite nanocrystals.	47
Figure 3.4	The range of ^{29}Si MAS NMR chemical shift for Si(nAl) species.....	52
Figure 3.5	The adsorption isotherms according to IUPAC classification.	55
Figure 4.1	XRD patterns of solid using a hydrogel molar composition of $4\text{SiO}_2:1\text{Al}_2\text{O}_3:x\text{Cs}_2\text{O}:164\text{H}_2\text{O}$ with (a) $x = 8$ (b) $x = 12$ and (c) $x = 16$. The synthesis were performed at $180\text{ }^\circ\text{C}$ for 80 min.....	63
Figure 4.2	XRD patterns of solid using a hydrogel molar composition of $4\text{SiO}_2:1\text{Al}_2\text{O}_3:16\text{Cs}_2\text{O}:z\text{H}_2\text{O}$ with (a) $z = 124$ (b) $z = 164$ and (c) $z = 204$. The synthesis were performed at $180\text{ }^\circ\text{C}$ for 80 min.....	64
Figure 4.3	XRD patterns of solid using a hydrogel molar composition of $y\text{SiO}_2:1\text{Al}_2\text{O}_3:16\text{Cs}_2\text{O}:164\text{H}_2\text{O}$ with (a) $y = 2$ (b) $y = 4$ and (c) $y = 6$. The synthesis were performed at $180\text{ }^\circ\text{C}$ for 80 min.	65
Figure 4.4	XRD patterns of solid using a hydrogel molar composition of $4\text{SiO}_2:1\text{Al}_2\text{O}_3:16\text{M}_2\text{O}:164\text{H}_2\text{O}$ with $\text{M} =$ (a) Na, (b) K and (c) Cs. The synthesis were performed at $180\text{ }^\circ\text{C}$ for 80 min.	66
Figure 4.5	XRD patterns of solid using a hydrogel molar composition of $4\text{SiO}_2:1\text{Al}_2\text{O}_3:16\text{Cs}_2\text{O}:164\text{H}_2\text{O}$ with different temperature for 80 min (a) $140\text{ }^\circ\text{C}$ (b) $160\text{ }^\circ\text{C}$ and (c) $180\text{ }^\circ\text{C}$	67
Figure 4.6	Yield of solids recovered after different time intervals of hydrothermal synthesis.....	68

Figure 4.7	XRD patterns of samples after heating for (a) 10 min, (b) 17 min, (c) 30 min, (d) 60 min and (e) 120 min. The theoretical XRD pattern reported in ref. (Gatta et al., 2008) is shown in (f).....	69
Figure 4.8	Degree of crystallinity of samples after heating for various times.....	70
Figure 4.9	TEM images of samples collected after hydrothermal treatment for (a, b) 10 min, (c, d) 17 min, (e, f) 30 min and (g, h) 120 min.	72
Figure 4.10	FTIR spectra of the solid after hydrothermal treatment for (a) 10 min, (b) 17 min, (c) 30 min and (d) 120 min.	74
Figure 4.11	²⁷ Al solid state MAS NMR spectra of the solid after hydrothermal treatment for (a) 10 min, (b) 17 min, (c) 30 min and (d) 120 min.	76
Figure 4.12	²⁸ Si MAS + DEC NMR spectra of the solid samples after hydrothermal treatment for (a) 10 min, (b) 17 min, (c) 30 min and (d) 120 min.	77
Figure 4.13	XRD patterns of (a) MW-2m, (b) MW-5m and (c) MW-6m solids.....	78
Figure 4.14	Rietveld refinement of the XRD pattern of ABW-type Cs-zeolite (MW-6m). Observed (solid line) and calculated (+ marks) XRD patterns, as well as the difference profile (bottom) are shown. Tick marks indicate peak positions. Inset: Crystal structure views along (a) a-direction (pore opening 8.23 × 4.39 Å ²), (b) b-direction (pore opening 8.23 × 4.39 Å ²) and (c) c-direction (pore opening 5.44 × 6.40 Å ²). Unit-cell is boxed. Purple: Cs, yellow: Si, pink: Al and red: O.	80
Figure 4.15	(a) SEM image and (b) DLS plot of Cs-ABW nanozeolites (MW-6m). Inset of (b) shows the TEM image of Cs-ABW zeolite nanocrystals.	84
Figure 4.16	Element distribution map (SEM/EDX) of nanocrystalline Cs-ABW (MW-6m).....	85
Figure 4.17	FTIR spectrum of nanocrystalline Cs-ABW solid (MW-6m).....	86
Figure 4.18	(a) TGA/DTG curves and (b) nitrogen gas adsorption (close symbols) and desorption (open symbols) isotherms of nanocrystalline Cs-ABW zeolite (MW-6m).	87
Figure 5.1	XRD patterns of (a) HT-10m (amorphous) and (b) HT-60m (zeolite Cs-ABW).....	90

Figure 5.2	(a) TEM and (b) SEM images of HT-60m (zeolite Cs-ABW) at different magnifications. Inset of (b): particle size distribution of HT-60m.	91
Figure 5.3	Nitrogen adsorption (close symbols) and desorption (open symbols) isotherms, and (inset) pore size distribution of HT-60m (zeolite Cs-ABW).	92
Figure 5.4	Element distribution map (SEM/EDX) of HT-60m (zeolite Cs-ABW).	93
Figure 5.5	TPD-CO ₂ plot of HT-60m (zeolite Cs-ABW) with deconvolution curves.	94
Figure 5.6	Appearance of reaction solution after subsequent reaction times	95
Figure 5.7	Effect of temperature on the conversion (a) 130 °C, (b) 140 °C, (c) 150 °C and (d) 160 °C. Catalyst (HT-60m) = 0.50 g, benzaldehyde = 2 mmol, nitroethane = 40 mmol, solvent free.	96
Figure 5.8	The linear plot derived from the Arrhenius equation for the nitroaldol reaction run (a) without catalyst and (b) with nanosized Cs-ABW zeolite.	97
Figure 5.9	Percentage of conversion of benzaldehyde of Henry reaction at different amounts of catalyst (HT-60m). Reaction temperature = 160 °C, time = 60 min, benzaldehyde = 2 mmol, nitroethane = 40 mmol, solvent free.	98
Figure 5.10	Percentage of conversion of benzaldehyde at different benzaldehyde:nitroethane molar ratios. Reaction temperature = 160 °C, time = 60 min, catalyst (HT-60m) = 0.50 g.	99
Figure 5.11	Percentage of conversion of benzaldehyde using different types of catalyst (1.984 mmol equivalent to 0.50 g ABW nanocatalyst). Reaction temperature = 160 °C, time = 60 min, benzaldehyde = 2 mmol, nitroethane = 40 mmol, solvent free.	102
Figure 5.12	Product conversion of nitroaldol from reusability test of HT-60 min (zeolite Cs-ABW).	106
Figure 5.13	TGA/DTG profiles of HT-60m (nanosized zeolite Cs-ABW) after catalytic reaction.	107
Figure 5.14	Nitrogen gas sorption isotherm plot of of HT-60m (nanosized zeolite Cs-ABW) after catalytic reaction.	107

Figure 5.15	TEM image of of HT-60m (nanosized zeolite Cs-ABW) after catalytic reaction.	108
Figure 5.16	Proposed mechanism of nitroaldol reaction of benzaldehyde with nitroethane catalyzed by Cs-ABW zeolite nanocatalyst.	109
Figure 6.1	XRD patterns of (a) A-1, (b) A-2 and (c) A-3 Cs-ABW zeolite nanocrystals.	113
Figure 6.2	(A) DLS and (B) zeta potential curves of (a) A-1, (b) A-2 and (c) A-3 Cs-ABW zeolite nanocrystals.	115
Figure 6.3	HRTEM images of (a–c) A-1, (d–f) A-2 and (g–i) A-3 samples at high and very high magnifications. Insets show the lattice fringes of single-crystal of Cs-ABW zeolite captured at selected square areas.	117
Figure 6.4	Nitrogen adsorption-desorption isotherms and (Inset) pore size distribution of (a) A-1, (b) A-2 and (c) A-3 Cs-ABW zeolite nanocrystals.	119
Figure 6.5	Total consumption of chemical reagents by conventional and recyclable synthesis methods for producing (a) 200 g of nanosized Cs-ABW zeolite in laboratory scale using 3 batches, and (b) 1 tonne of nanosized Cs-ABW zeolite in industry scale (estimated) using 100 batches.	120

LIST OF ABBREVIATIONS, NOMENCLATURES AND SYMBOLS

°C	Degree Celsius
Al	Aluminum
Å	Angstrom (1×10^{-10} m)
AlO ₄	Aluminum tetraoxide
Al(OH) ₃	Aluminum hydroxide
ca.	Circa (approximately)
DLS	Dynamic light scattering
FESEM	Field emission scanning electron microscopy
EDI	Edingtonite
F ⁻	Fluoride ion
SEM	Scanning electron microscopy
FTIR	Fourier transform infrared spectrophotometer
g	gram
H ₂ SO ₄	Sulfuric acid
HCl	Hydrochloric acid
HNO ₃	Nitric acid
HRTEM	High resolution transmission electron microscopy
h	Hour
IZA-SC	International Zeolite Association Structure Commission
KBr	Potassium bromide
KOH	Potassium hydroxide
M	Molarity
MAS NMR	Magic angle spinning nuclear magnetic resonance
min	Minute

NaOH	Sodium hydroxide
NH ₄ OH	Ammonium hydroxide
nm	nanometer (1×10^{-9} m)
O ₂	Oxygen
OH ⁻	Hydroxide ion
PBU	Primary building unit
PP	Polypropylene
PSA	Pressure swing adsorption
ppm	Part per million
S _{BET}	BET surface area
SAED	Selected area electron diffraction
SBU	Secondary building unit
SDAs	Structure-directing agents
Si	Silicon
SiO ₂	Silicon dioxide
SiO ₃ ²⁻	Silicate ion
SiO ₄	Silicon tetraoxide
TGA/DTA	Thermogravimetric and differential thermal analysis
TEOS	Tetraethylorthosilicate
TMA	Tetramethylammonium
TPA	Tetrapropylammonium
VOCs	Volatile organic compounds
wt%	Weight percentage
XRD	X-ray diffraction

**KAJIAN SINTESIS, PENCIRIAN DAN PEMANGKINAN ZEOLIT Cs-ABW
NANOHABLUR DALAM TINDAK BALAS HENRY BENZALDEHID
DENGAN NITROALKANA**

ABSTRAK

Zeolit Cs-ABW merupakan zeolit aluminosilikat berliang gelang 8 ahli (diameter $3.4 \times 3.8 \text{ \AA}^2$) yang jarang dilaporkan dalam penggunaannya kerana keadaan penghablurannya yang merbahaya dengan suhu dan tekanan yang tinggi ($695 \text{ }^\circ\text{C}$, 1000 bar). Dalam projek ini, zeolit Cs-ABW nanohablur telah berjaya disintesis secara hidrotermal tanpa sebarang acuan organik merbahaya. Zeolit nanohablur tersebut dengan hasil pepejal yang sangat tinggi (81.88%) boleh diperolehi dalam masa 60 min pada $180 \text{ }^\circ\text{C}$ ($\sim 20 \text{ atm}$), iaitu suatu keadaan yang lebih cepat dan lembut berbanding kaedah sintesis yang sedia ada. Cs-ABW nanohablur yang berbentuk ortorombik (saiz min 32 nm) mempunyai kandungan aluminium yang tinggi (nisbah Si/Al = 1.14) dan mempunyai kebesaran yang tinggi. Selain itu, zeolit Cs-ABW nanohablur (sekitar 68 nm) juga disintesis di bawah pemanasan gelombang mikro yang telah memendekkan masa penghabluran dengan ketara kepada 6 min pada $180 \text{ }^\circ\text{C}$. Nanohablur yang disintesis dengan kedua-dua kaedah ini menunjukkan prestasi pemangkinan yang lebih baik daripada mangkin homogen biasa dalam tindak balas Henry (nitroaldol) benzaldehid dengan nitroalkana di bawah keadaan pemanasan segera gelombang mikro dan bukan gelombang mikro. Mangkin nano tersebut mempunyai kebolegunaan semula yang tinggi dan tidak mengalami masalah pengekokan dan larut lesap kerana ia boleh diguna semula tanpa kehilangan kereaktifan walaupun selepas lima kitaran tindak balas konsekutif. Selain itu, projek ini juga tertumpu kepada sintesis zeolit Cs-ABW nanohablur berhasil tinggi, murah dan secara hijau

dengan mengitar dan menggunakan semula likuor ibu yang tidak ditindak balaskan yang dihasilkan daripada sintesis hidrotermal Cs-ABW zeolit. Cs-ABW nanohablur yang diperoleh daripada tiga set sintesis yang berturutan mempunyai hampir sama saiz (sekitar 31 nm) dan ciri-ciri fizikokimia (luas permukaan, isipadu liang, komposisi kimia, kestabilan koloid dan sebagainya). Selain itu, mangkin nano ini juga mempunyai keaktifan pemangkinan yang hampir sama dalam tindak balas nitroaldol benzaldehid dengan nitroalkana.

**SYNTHESIS, CHARACTERIZATION AND CATALYTIC STUDIES OF
NANOCRYSTALLINE Cs-ABW ZEOLITE IN HENRY REACTION OF
BENZALDEHYDE AND NITROALKANES**

ABSTRACT

Zeolite Cs-ABW is an 8-membered ring pore aluminosilicate zeolite (diameter of $3.4 \times 3.8 \text{ \AA}^2$) that is rarely reported in its application due to its dangerous crystallization condition using high temperature and pressure (695 °C, 1000 bar). In this work, zeolite Cs-ABW nanocrystals have been hydrothermally synthesized without using any harmful organic template. The zeolite nanocrystals with very high solid yield (81.88%) can be obtained within 60 min and at 180 °C (~20 atm); a condition which is much faster and gentle than the existing synthesis methods. The orthorhombic shaped Cs-ABW nanocrystals (mean size of 32 nm) have high aluminum content (Si/Al ratio = 1.14) and possess high basicity. In addition, Cs-ABW zeolite nanocrystals (ca. 68 nm) was also synthesized under microwave heating condition where microwave energy significantly shortened the crystallization time to 6 min at 180 °C. The nanocrystals synthesized using both methods exhibited better catalytic performance than the conventional homogeneous catalysts in Henry (nitroaldol) reaction of benzaldehydes with nitroalkanes under microwave and non-microwave instant heating conditions. The nanocatalysts have high reusability and do not suffer from coking and leaching problems because they can be reused without loss of reactivity even after five consecutive runs under the described reaction conditions. Furthermore, this project is also focused on the high-yield, low-cost and green synthesis of nanosized Cs-ABW zeolite by recycling and reusing the non-reacted mother liquors which are produced from the hydrothermal Cs-ABW zeolite synthesis.

The Cs-ABW nanocrystals of three successive batches have almost similar sizes (ca. 31 nm) and physicochemical properties (surface area, pore volume, chemical composition, colloidal stability, etc.). In addition, these nanocatalysts also have almost similar catalytic activity in nitroaldol reaction of benzaldehyde with nitroalkane.

CHAPTER ONE

INTRODUCTION

1.1 General introduction

Zeolites are crystalline aluminosilicates which contain many channels and cavities. They are constructed from $[\text{AlO}_4]^{3-}$ and $[\text{SiO}_4]^{4-}$ tetrahedral units that are linked to each other by sharing oxygen atoms (Stocker et al., 2017). The cavities contain molecular water while monovalent or divalent cations are also present as extraframework cations to balance the negative charge of the framework of zeolites after substituting tetravalent silicon by trivalent aluminum (Motsi et al., 2009). The International Zeolite Association (IZA) recently has identified 235 types of zeolite structures (Baerlocher and McCusker, 2019). Natural zeolite was first discovered in 1756. Until now, more than 40 types of natural zeolites with different pore sizes (3 to 12 Å) are discovered (Hovhannisyanyan et al., 2018).

Zeolites are thermally stable and their properties do not change under high temperature and pressure. Furthermore, zeolites have very low toxicity and high surface area due to their porous nature (Kasperkowiak et al., 2016). Because of these features, zeolites have been used in many applications such as in catalysis (Amodu et al., 2015), biomedicine as drug delivery agents (Anderson et al., 2017), environment as adsorbents to remove heavy metals from wastewater (Bashir et al., 2018), agriculture as fertilizer (Pavlovic et al., 2017) and so on. The suitable applications of zeolites depend on the dimensions of pores, shapes and crystal sizes of zeolites (Moliner et al., 2015). However, the big obstacles in zeolite catalysts are diffusion of bulkier reactants and products in their micropores that leads to pore blockage and

deactivation of the catalysts. In order to solve this problem, the particle size of zeolites is reduced to the nanometer scale (Mintova et al., 2016).

Recently, the synthesis, characterization and applications of nanometer-scale zeolites (<100 nm) have received intense attentions due to their more unique and fascinating properties, such as reducing diffusion path length, high colloidal stability, large external surface area and surface active sites of zeolite, low toxicity, high activation and stabilization of host molecules in the pore channels and on the external surface of zeolites, as compared to the micron-sized zeolites (Wong et al., 2017; Huang et al., 2017). As a result, these unique properties allow the expansion of the area of zeolite applications toward atomic energy production (Chica, 2013), food (Eroglu et al., 2017), paper (Mateena et al., 2015), drug delivery (Rimoli et al., 2008), ceramics (Adam et al., 2017), paints (Cheng et al., 2001), electronics (Herron, 1995), recording materials (Gul et al., 2018), lubricants (Zaarour et al., 2019), and detergents (Carran et al., 2015).

Usually, zeolite nanocrystals are synthesized by adding organic templates or so-called structure-directing agents (SDAs) (amine, imidazolium or quaternary ammonium salts) to the aluminosilicate precursor solutions (Ng et al., 2014; Song et al., 2005). The organic templates are used to control the size of crystals, and to synthesize zeolites with specific crystalline frameworks through structure-directing mechanism. However, there are several disadvantages of using organic templates. First, the organic template has to be removed by calcination at high temperature after the synthesis of nanozeolites and it may lead to irreversible aggregation. Second, the use of organic templates during the hydrothermal synthesis of nanozeolites causes a change in the framework composition and surface hydrophilicity/hydrophobicity. For example, the zeolite A (LTA topology) with a Si/Al ratio >1 is obtained when the

synthesis is carried out using organo-template approach, but the Si/Al ratio = 1 when no organo-template is applied. Thus, this leads to the change in the framework properties and affecting their applications. Third, some organic templates made up of quaternary ammonium and N-heterocyclic compounds are expensive and harmful to environment and living organisms (Duan et al., 2018; Cui et al., 2017).

There are many methods to synthesize nanosized zeolites to become more eco-friendly and less costly such as ionothermal (Khoo et al., 2013), confined space synthesis (Wang et al., 2003), seed-induced (Kamimura et al., 2011; Shi et al., 2018), post-milling recrystallization (Wakihara et al., 2011; Yamada et al., 2016), and organic template-free synthesis methods (Ng et al., 2015; Wang et al., 2017). Of note, the last approach is the most interesting since no organic template is used and it is much simple as compared to the other methods. As a result, organotemplate-free method offers cheaper production cost in large scale process in industry.

The organotemplate-free synthesis of zeolites using sodium and potassium is widely reported. For example, zeolites FAU, SOD, LTA, EMT are crystallized in sodium-rich precursors (Oleksiak, M. D., & Rimer, 2014, Ogura et al., 2003; Tosheva and Valtchev, 2005) while zeolites LTL, LTJ, EDI and MER are formed in potassium-rich aluminosilicate hydrogels (Ahmad et al., 2020; Thomas et al 2017; Cheong et al., 2018). However, cesium as a mineralizer is rarely reported due to its dangerous and impractical synthesis condition where only two reports on the formation micron-sized ABW zeolite (>50 μm) templated by Cs^+ cation were reported (Klaska et al., 1973; Klaska et al., 1975) in 1970s. Unlike Li-ABW, the system using Cs^+ cation required extremely high temperature (700-1200 $^{\circ}\text{C}$) and pressure (>1000 bar) with considerably long crystallization time (46 h). Also, the preparation of cesium-based zeolite nanocrystals using this method has never been reported so far. It is because the

synthesis of zeolite nanocrystals is a complicated process because it is affected by many parameters such as sources of alumina and silica used, synthesis temperature, crystallization time, type and concentration of alkali metal mineralizer, water content, aging, and heating mode. Hence, a comprehensive study on the synthesis of cesium-based nanozeolites and investigation of nucleation and crystallization steps are worth to be further explored.

Zeolite containing Cs^+ cation is very interesting due to its highly basic property that is appreciated in base-catalyzed reactions such as Knoevenagel condensation, Michael condensation, Henry condensation reaction and cyanoethylation reaction (Zamanian and Kharat, 2014; Ballini et al., 2000; Cheng et al., 2010).

Particularly, Henry (nitroaldol) reaction offers β -nitroaldol as the condensation product which can be transformed into compounds like aminoalcohols, aminoketones, nitroalkenes, and thus act as versatile intermediates for synthesis of various biological, pharmaceutical and fine chemical products (Fabris et al., 2012). This reaction is widely studied in homogeneous catalysis system, but not investigated in heterogeneous catalysis system.

In this study, the synthesis of nanozeolite with ABW topology in cesium-rich and organotemplate-free medium is reported. The mechanism of the formation of Cs-ABW zeolite nanocrystals and the effects of synthesis parameters on crystallization process are investigated. In addition, this work is also dedicated on the design of greener synthesis of Cs-ABW zeolite nanocrystals by using the non-reacted solution to recrystallize this zeolite with an aim to achieve the target of green chemistry. Lastly, the catalytic behavior of Cs-ABW nanozeolite in base-catalyzed reactions such as nitroaldol condensation of benzaldehyde reaction is tested.

1.2 Research objectives

- a) To synthesize and to study the formation of Cs-ABW zeolite nanoparticles (<100 nm) free of organic template under conventional hydrothermal and microwave-assisted hydrothermal conditions.
- b) To investigate the effects of synthesis parameters on the formation of Cs-ABW zeolite nanocrystals.
- c) To design a new green synthesis approach for nanosized Cs-ABW zeolite by recycling and reusing the non-reacted aluminosilicate mother liquor.
- d) To study the catalytic behavior of Cs-ABW zeolite nanocrystals in base-catalyzed nitroaldol (Henry) reaction of benzaldehydes and nitroalkanes using microwave and/or non-microwave instant heating methods.

1.3 Overview of the thesis

This thesis is composed of seven chapters that cover the background, experimental procedures and research findings of the project.

Chapter 1 is an introduction dedicating to the definition, properties and applications of (nano)zeolites. The problem statements, objectives and overview of this work are also covered in this chapter too.

Chapter 2 is a comprehensive literature review describing the history of zeolites, zeolite framework structures and properties, the fundamental concepts of (nano)zeolite synthesis and their applications specifically in heterogeneous catalysis.

Chapter 3 presents the experimental methodology used in this study where the formation of nanosized Cs-ABW zeolite using conventional hydrothermal and microwave-assisted hydrothermal techniques is reported. In addition, the synthesis procedure of nanosized Cs-ABW zeolite by recycling and reusing the non-reacted

aluminosilicate mother liquor is also described in this chapter. Furthermore, the information on the analysis set-up for characterization of samples, such as X-ray diffraction analysis (XRD), Fourier transform infrared spectroscopy (FT-IR), nitrogen sorption isotherm analysis, thermogravimetry and differential thermogravimetry analysis (TG/DTG), solid state nuclear magnetic resonance spectroscopy (^{27}Al , ^{29}Si MAS NMR), inductively coupled plasma atomic emission spectroscopy (ICP-OES), field emission scanning electron microscopy (FESEM), energy-dispersive X-ray spectroscopy (EDX), nitrogen adsorption analysis, temperature program desorption of carbon dioxide (TPD- CO_2) analysis, gas chromatography (GC), and gas chromatograph-mass spectrometry (GC-MS), are also detailed in this chapter.

Chapter 4 presents the results of the synthesis and formation study of nanosized Cs-ABW zeolite free of organic template under conventional and microwave-assisted hydrothermal conditions. In this chapter, the effects of synthesis conditions, such as heating time, temperature, type and concentration of mineralizers (NaOH, KOH and CsOH), water content and silica concentration, on the nucleation and crystal growth of Cs-ABW nanozeolite are investigated. The solid samples were analyzed by using various characterization techniques such as XRD, TEM, ^{29}Si and ^{27}Al solid state NMR spectroscopy, FT-IR spectroscopy and ICP-OES elemental analysis.

Chapter 5 focuses on the catalytic behavior of Cs-ABW nanozeolite. Nitroaldol condensation (Henry) reaction of benzaldehydes with nitroalkanes is chosen as a model reaction where the reaction is conducted under microwave irradiation. The reaction products are evaluated with gas chromatograph equipped with flame ionization detector (GC-FID). Furthermore, the catalytic reaction parameters, such as heating temperature, time, solvents, catalyst loading, type of catalyst, reactants ratio, heating method, effect of benzaldehyde derivatives and chain length of nitroalkane,

and catalyst reusability, on the catalytic performance of Cs-ABW nanocatalysts are also reported. The mechanism this organic reaction catalyzed by Cs-ABW nanozeolite is also elucidated at the end of this chapter.

Chapter 6 reports the results of the design of a new green synthesis approach of nanosized Cs-ABW zeolite by recycling and reusing the non-reacted aluminosilicate mother liquor. The non-reacted mother liquor after Cs-ABW zeolite synthesis, which is normally discarded to the environment, is reused for the subsequent cycles of synthesis of Cs-ABW zeolite after careful chemical compensation is made. By using this approach, the consumption of chemicals and the production of chemical waste can be reduced to a very large extent, offering zero-waste options for the existing synthesis methods. The solid sample is analyzed by using various characterization techniques such as XRD, HRTEM, FT-IR, ICP-OES, TG/DTG, N₂ adsorption-desorption, dynamic light scattering (DLS) and zeta potential analyses.

Chapter 7 concludes the research findings. Furthermore, the recommendations for the future work of this research are also given at the end of this chapter.

CHAPTER TWO

LITERATURE REVIEW

2.1 Introduction of zeolites

Zeolites are hydrated microporous tectosilicates with crystalline structures. This mineral (stilbite) was first discovered by a mineralogist, Axel Fredrik Cronstedt, in 1756 (Cronstedt and Beskriting, 1756). The term zeolite comes from two Greek words: "zeo" which means boiling and "lithos" means stone because this mineral looks boiling when it is heated above 150 °C.

Basically, the framework of zeolite is constructed from three dimensional tetrahedra of Al ($[\text{AlO}_4]^{3-}$) and Si ($[\text{SiO}_4]^{4-}$) where the oxygen atoms are linked them together forming primary building units of zeolites (Weckhuysen and Yu, 2015). The basic building units of zeolites in most cases have negatively charge. In order to balance the surface charge, inorganic (alkaline or alkaline earth metals: Na^+ , K^+ , Li^+ , Cs^+ , Ca^{2+} , etc.) or organic (quaternary alkylammonium) cations are introduced to the external surface of zeolites *via* electrostatic forces (Figure 2.1) (Jha, B., & Singh, 2016).

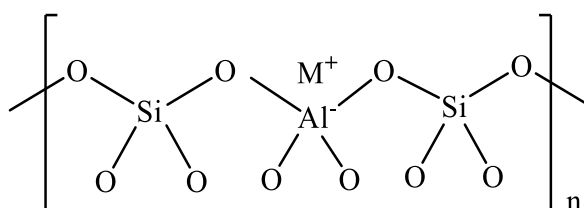
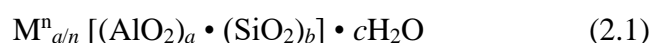


Figure 2.1. The basic structure of zeolites with n repeating units where negative charge of Al site is charge balanced by metal cations (M^+).

Upon polymerization of these Si and Al tetrahedra in three-dimensional arrangement, many varieties of channels, cages and pores that are readily occupied by water, organic and metal cations can be created (Büchner and Heyde, 2017). The

adsorbed organic and water molecules can be removed *via* heat treatment. On the other hand, the extra-framework cations electrostatically interacted with surface framework are mobile and can be replaced by other cations using ion exchange process (Marakatti and Halgeri, 2015).

The chemical formula of zeolites can be simplified and presented in Equation 2.1 (Auerbach et al., 2003; Yuna, 2016).



where M is the organic or inorganic cation with n charge, *a* and *b* are the numbers of tetrahedral units, and *c* is the number of water molecules chemisorbed by the zeolites (Yuna, 2016).

Zeolites are classified according to their ring size and pore diameter which determine their applications in industries (Figure 2.2) (Moshoeshoe et al., 2017). Zeolites have 4-, 5-, 6-, 8-, 10-, or 12-membered rings (MR) where 4-, 5-, 6- and 8-MR are classified as small pore zeolites (2-4 Å), while 10-MR and 12 MR have medium (5.5 Å) and large (7.7 Å) pores, respectively (Auerbach et al., 2003). In addition, the zeolites framework can also be classified according to the number of channel dimensions. The zeolites with 1-dimensional pore channel has an opening at one direction whereas zeolites with 2- and 3-dimensional pore channels have multi-opening at two and three axes, respectively (Moliner et al., 2015). Figure 2.3 shows some zeolites with different pore sizes and pore channels (Schwanke et al., 2017).

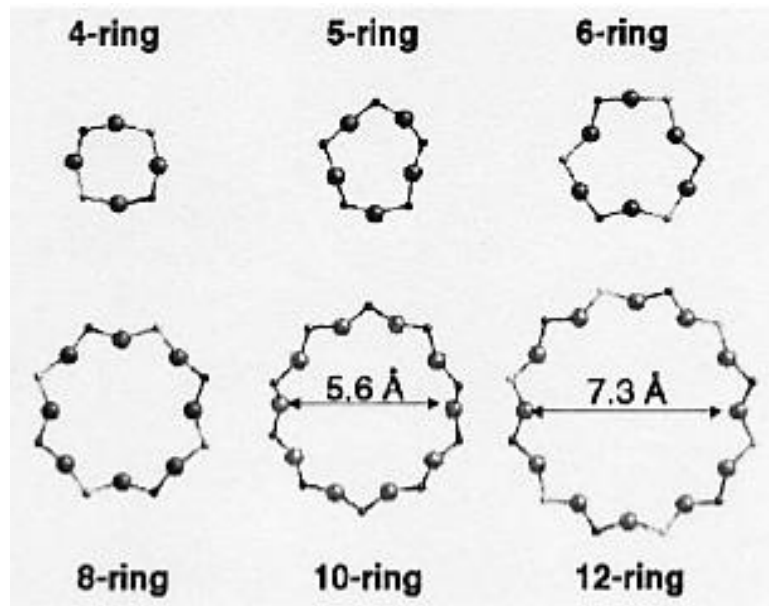


Figure 2.2. Ring size of zeolites.

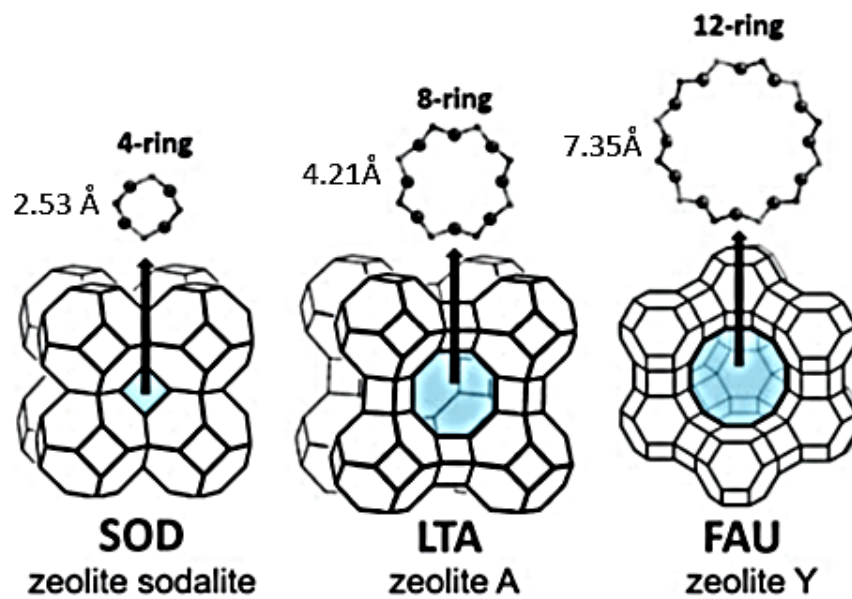


Figure 2.3. Some examples of zeolites with different pore sizes and pore dimensions (Schwanke et al., 2017).

Furthermore, zeolites can also be classified based on their aluminum content in the zeolite framework where it is well described by referring to their Si/Al ratio. For instance, low-silica zeolites such as zeolite X, sodalite, A and P have a Si/Al ratio ≤ 2 , whereas intermediate silica zeolites such as zeolite Y, EMC-2 and offretite have a

Si/Al ratio between 2 to 5 and high silica zeolites such as ZSM-5 and Beta have a Si/Al ratio >5 (Yang et al., 2018).

2.2 Zeolite structures and properties

The framework structures of zeolites are basically constructed by the primary and secondary building units (Figure 2.4). The primary building units (PBUs) are $(\text{AlO}_4)^{4-}$ and/or $(\text{SiO}_4)^{4-}$ tetrahedra. These PBUs are linked together by sharing O atoms and form secondary building units (SBUs). The combination of SBUs produces different ring shapes such as single 4- and 6- rings (S4R, S6R), double 4- and 6-rings (D4R, D6R), polyhedral or even more complex units which are connected together to form a new system of cages and channels, and finally producing zeolites with different frameworks (Baerlocher et al., 2007). Today, there are about 23 types of SBUs known in forming zeolite frameworks (Zhai et al., 2017). However, PBUs and SBUs are not enough to describe the framework of zeolites because of the complexity of the zeolite frameworks during that time. Hence, the researchers used composite building units (CBUs) to describe the structure of the zeolite. In general, CBUs are formed by a combination of the rings, cages and channels where the size of the rings (4-, 5-, 6-, 8-, 10- and 12-MR) is determined by the number of Si and/or Al tetrahedra (Hay, 1986). The cages are formed when two channels are crossed and these cages allow the molecules to pass through. On the other hand, the cages linked together become pores by which the pore size less than 2 nm is called micropores (Xu et al., 2007; Shin et al., 2019).

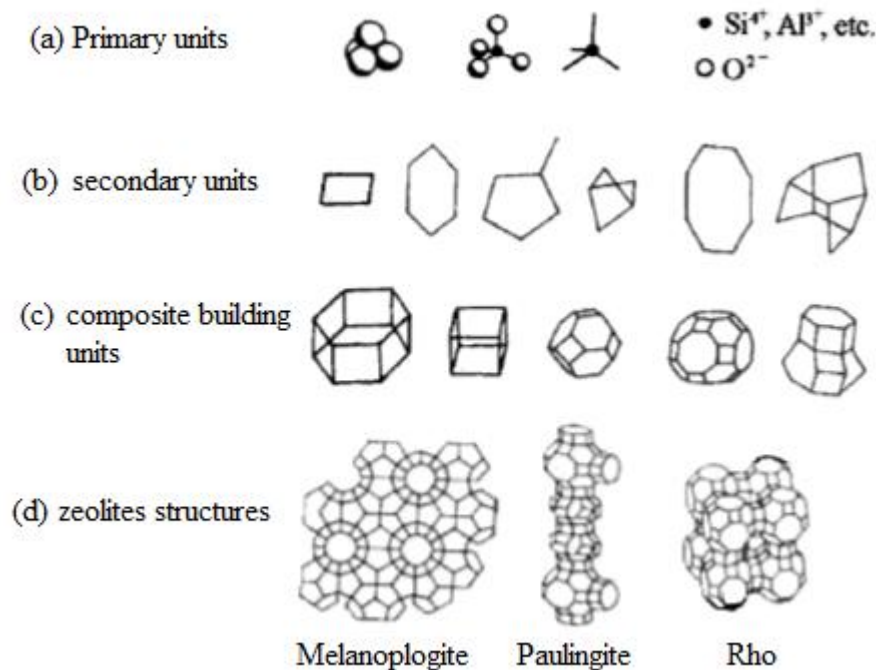


Figure 2.4. (a) Primary building units (PBUs): $(\text{SiO}_4)^{4-}$ or $(\text{AlO}_4)^{5-}$, (b) secondary building units (SBUs), (c) composite building units (CBUs), and (d) structures of zeolites (Auerbach et al., 2003).

2.3 Nomenclature of zeolites

Meier and Olson compiled the classification of zeolites based on the framework type of zeolites in a book (Meier and Olson, 1978). The classifications depend on the type of minerals and/or the name of zeolites. All of these zeolite frameworks are given a specific code containing three capital letters. Today, the International Zeolite Association (IZA) is the organization who is responsible to produce and assign the codes to the newly discovered zeolite framework structures.

The nomenclature of the zeolite frameworks depends on three conditions (Byrappa and Yoshimura, 2013). First, it is according to the names of minerals which have the same framework structure as the zeolites where these rules are followed and applied by the International Mineralogical Association. Second, the nomenclature is

based on the known synthetic material types. Third, if the framework structures are not found in the existing framework database, the researchers or research groups who first discovered the framework structure have privilege in giving the name for the framework structure. Table 2.1 illustrated some names of zeolite framework structures (http://europe.iza-structure.org/IZA-SC/Zeolite_names.html#L).

Table 2.1

Some examples of structure types.

Codes	Materials	Full names
ABW	Li-ABW	Li-A (Barrer and White)
ACO	ACP-1	Aluminium Cobalt Phosphate Number One
AEL	AIPO-11	Aluminophosphate Number Eleven
AFR	AIPO-40	Aluminophosphate Number Forty
CDO	CDS-1	Cylindrically Double Saw-edged Structure Number One
LTA	Zeolite A	Linde Type A
MEL	ZSM-11	Zeolite Socony Mobil Number Eleven
MFI	ZSM-5	Zeolite Socony Mobil Five
MFS	ZSM-57	Zeolite Socony Mobil Number Fifty Seven
MSO	MCM-61	Mobil Composition of Matter Number Sixty One
MTF	MCM-35	Mobil Composition of Matter Number Thirty Five

2.4 Formation of zeolites

Recently, the zeolite scientists are interested in studying the mechanism of the formation of zeolite with an aim to synthesize zeolites with new structures and improved properties. In general, the zeolite formation involves nucleation and crystallization. Cundy et al. (Cundy and Cox, 2005) and Cubillas et al. (Cubillas and Anderson, 2010) are the research groups that described the mechanism of zeolite formation in details. In nucleation process, it consists of sequential steps such as

prenucleation, primary nucleation and secondary nucleation where the supersaturating phenomenon occur during prenucleation step (Figure 2.5). This phenomenon is important and responsible for the early formation of zeolites. Generally, the prenucleation step experiences partial/complete dissolution of Al and Si sources forming amorphous in the form of dimers, trimers and/or oligomers. After dissolution, the concentration of soluble Si and Al species in precursor increases and a supersaturation condition is reached (Masoumifard et al., 2018). The primary nucleation occurs in an amorphous phase and the chemical process is not in equilibrium due to the high free energy of the system. As a result, the solid with heterogeneous amorphous phases is usually formed. When the mixtures undergo heating at a specific time under controlled conditions, secondary nucleation step begins whereby the reaction reaches equilibrium and an aggregation of small-sized nuclei takes place forming a reactive intermediate (Aerts et al., 2010; Cundy and Cox, 2005). Upon prolonging heating time with constant temperature, the amorphous solids undergo rearrangement, aggregate to form the big size of zeolite crystals with distinct shapes (Grand et al., 2016).

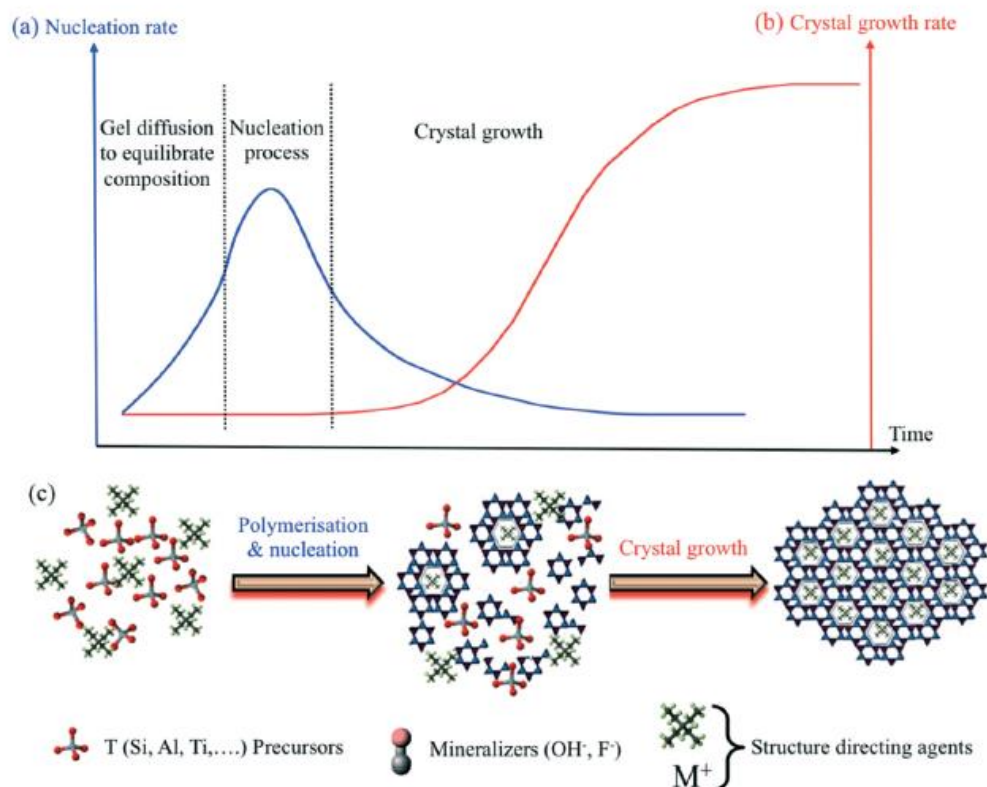


Figure 2.5. The kinetics of (a) nucleation and (b) crystal growth of zeolites, and (c) the mechanism of the conversion of amorphous particles into crystalline zeolite framework (Grand et al., 2016).

2.5 Synthesis of zeolites

Zeolites can be synthesized in the laboratory by using various methods where hydrothermal and solvothermal methods are the most popular ones. The synthesis methods are very important as it governs the properties and morphology of zeolite despite the type of the initial reactants composition, type of reactants and the crystallization conditions (Xu et al., 2007). Basically, the difference between hydrothermal and solvothermal synthesis is that the hydrothermal method uses an aqueous medium for crystallizing zeolites while the solvothermal method uses a non-aqueous medium (Feng and Li, 2017). In fact, both the hydrothermal and solvothermal methods can improve the growth of zeolite crystals by simply controlling the

crystallization conditions where both techniques provide suitable pressure (1-50 bar) and temperature (100-240 °C) to allow the reactants to react and form the zeolite crystals (Rao et al., 2017).

The synthesis of zeolites can be divided into several steps as shown in Figure 2.6 (Grand et al., 2016). Firstly, it involved the mixing of the reactants to obtain amorphous gel or precursor mixture where polymerization and depolymerization of silicate and aluminate species occur concurrently until an equilibrium is achieved (Aerts et al., 2010). Next, it proceeds with the crystallization where the resulting hydrogel mixture is transferred to a Teflon autoclave and heated at a specific temperature with various times. Third, the mother liquor after completion of crystallization is filtered, washed and dried (Li et al., 2015). In some cases, organic templates are used during the synthesis of zeolites and hence, the last step is to calcine the as-synthesized zeolite product at high temperature in order to remove the organic template (Martínez-Franco et al., 2016).

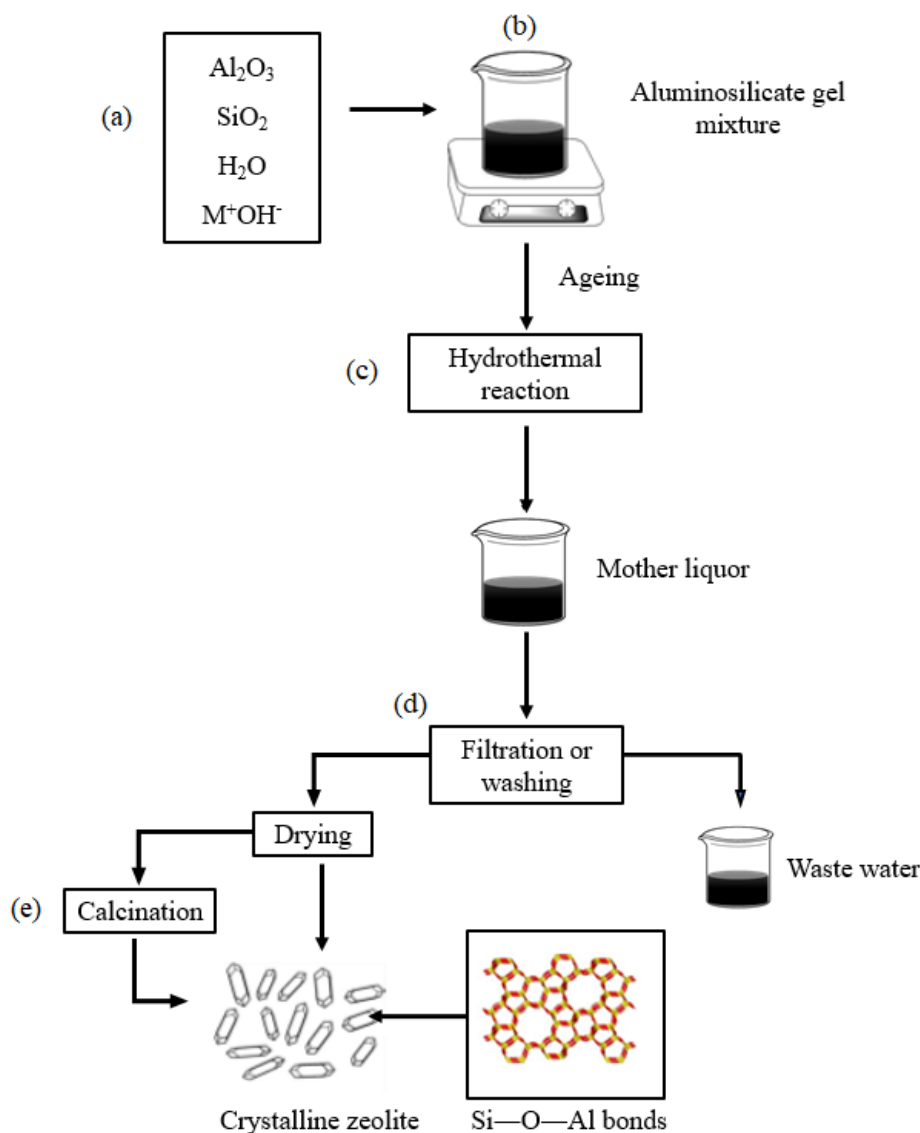


Figure 2.6. Processes of zeolite synthesis: (a) selection of initial chemical reagents, (b) preparation of precursor mixture (dense gel or colloidal suspension), (c) crystallization of zeolites, (d) purification, and (e) calcination of as-synthesized zeolite crystals.

2.6 Effect of synthesis parameters on the formation of zeolites

There are many factors influencing the formation of zeolite during synthesis process, including crystallization time and temperature, mineralizing agents, source of silica and alumina, Si/Al ratio of precursor hydrogel, water content, type of structure-directing agent and the presence of seed. In fact, they play a role to determine the type,

morphology and topology of zeolite and also effect on the properties. The most important to control these factors to synthesize and determine the behavior of zeolite.

2.6.1 Sources of silica and alumina

The type/source of initial reactants can have significant influences on the properties and framework structure of zeolites formed (Grand et al., 2016). Particularly, the silica source plays a very crucial role in the nucleation and crystallization processes where the selection of specific silica sources can lead to the formation of zeolites with different framework structures and crystal sizes (Tekin et al., 2015). The silica reactants with different surface area, in particular, have different surface energies and hence they affect very much on the initial dissolution process, crystallization rate and crystal sizes. For example, fumed silica with high surface area is much easier to be dissolved in the alkaline precursor hydrogel than that of low surface area due to its abundance silanol group (high surface energy). Such dissolution process leads to supersaturation condition which promotes fast nucleation that favors the formation of small crystals. In contrast, the fumed silica source with a low surface area has low solubility in the precursor solution, forming large zeolite crystals (Oleksiak and Rimer, 2014). In addition, the silica source also influences the framework structure of zeolites formed. One good example is by using sodium silicate and colloidal silica as the comparative silica sources. If sodium silicate is used during the synthesis, hydroxysodalite (SOD) and P (ANA) type zeolites are obtained as the final products. However, chabazite (CHA) and gmelinite (GME) are formed if colloidal silica is employed as a silica source (Xu et al., 2007). The common silica sources used in the synthesis of zeolites are fumed silica, water glass, colloidal silica, sodium silicates, precipitated silica and alkoxy silanes (e.g. tetraethylorthosilicate).

The alumina sources are also an important parameter in synthesizing zeolite materials. Some commonly used Al sources are aluminum hydroxide ($\text{Al}(\text{OH})_3$), pseudoboehmite (AlOOH), aluminum metal (Al), sodium aluminate (NaAlO_2), aluminum sulfate ($\text{Al}_2(\text{SO}_4)_3$), aluminum nitrate ($\text{Al}(\text{NO}_3)_3$) and aluminum isopropoxide ($\text{Al}(\text{OiPr})_3$) (Cejk et al., 2017). The aluminum sources influence directly the pH of the solution due to its amphoteric nature. For example, $\text{Al}_2(\text{SO}_4)_3$ has a pH equals to 3.8 while the pH value of $\text{Al}(\text{NO}_3)_3 \cdot 9\text{H}_2\text{O}$ is 2.5. However, the pH values increased to 6.1 and 11.4 for $\text{Al}(\text{OH})_3$ and NaAlO_2 solutions, respectively (Salou et al., 2001).

Zhang et al. explained the effect the aluminum sources ($\text{Al}(\text{OH})_3$, NaAlO_2 , AlOOH) on the particle size of ZSM-5/ZSM-11 (Zhang et al., 2012). They found that the selection of an aluminum source has an influence on the Si/Al ratio of the zeolite products because these Al sources have different Al releasing rate from the compounds as a result of their different dissolution ability and chemical properties. Based on their study, the Al solubility power follows this order: NaAlO_2 solution (30–40%) < $\text{Al}(\text{OH})_3$ solution (60–70%) < AlOOH solution (80–90%) (Dědeček et al., 2019; Zhang et al., 2012).

2.6.2 Effect of the Si/Al ratio

The values of Si/Al ratio in precursor hydrogels can be tailored ranging from 1 to ∞ (pure siliceous). It has very significant influences on the type, structure, characters and size of zeolites (Shalygin et al., 2017). For instance, the Si/Al ratio governs the thermal stability of a zeolite where its stability is enhanced with increasing the ratio. In addition, the low silica zeolites (which have high Al content) are energetically unstable because of their high surface negative charge originating from the

framework $[\text{AlO}_4]^-$ that leads to electrostatic repulsion. Usually, Al-rich zeolites are prepared in the precursor hydrogels containing low Si/Al ratio under strong alkaline environment while the zeolite with low Al content is prepared in weak alkaline solution (Johnson and Arshad, 2014).

2.6.3 Alkalinity

Zeolites are normally synthesized under basic conditions where the degree of basicity is depending on the molar ratio of OH^-/Si and $\text{H}_2\text{O}/\text{Na}_2\text{O}$. The alkalinity is an important parameter because it controls the solubilization of Si and Al sources. An increase in the alkalinity leads to the increase of the solubility of Si and Al sources, and accelerates the polymerization of the silicates and aluminates. In addition, high alkalinity of the precursor hydrogels also speeds up the rates of induction and nucleation, and then accelerates the crystallization of zeolites (Figure 2.7) (Xu et al., 2007). As a result, the zeolite crystals with smaller crystallite size and narrow particle size distribution are formed thanks to the increase in the rate of polymerization of silicate and aluminate, and nucleation rate (Johnson and Arshad, 2014). Moreover, the precursor solutions with strong alkalinity is essential for crystallizing Al-rich zeolites (Si/Al ratio < 2) such as FAU, ABW, SOD and GIS typed zeolites. On the other hand, zeolites are very rarely crystallized under acidic condition because high pH is needed to dissolve Al and Si sources (Dou et al., 2010).

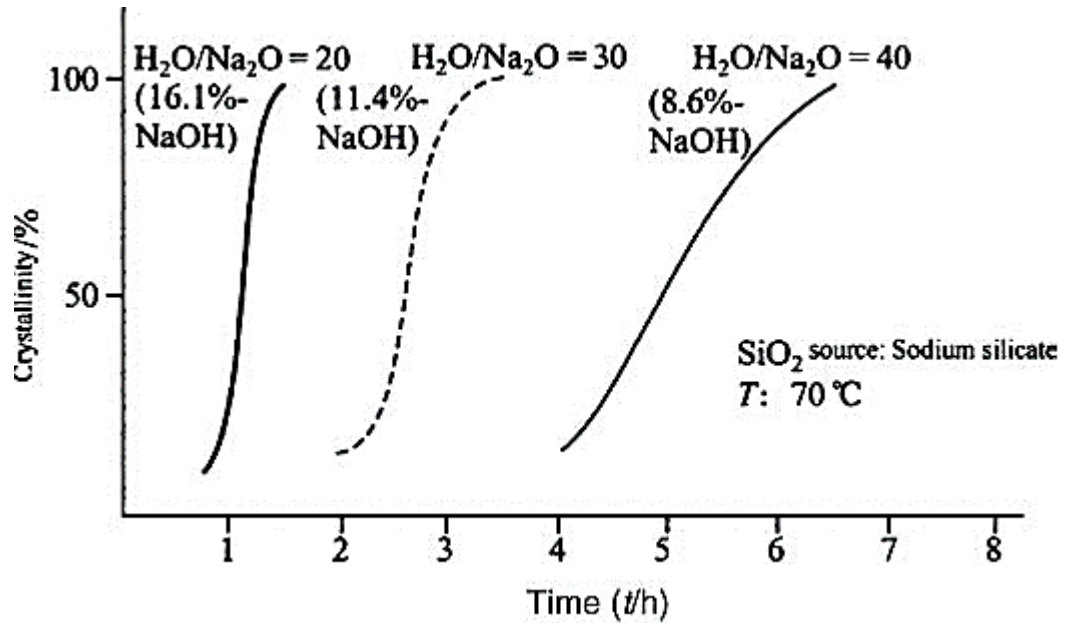


Figure 2.7. Crystallization kinetics of zeolite A influenced by the alkalinity of the precursor hydrogel of $5\text{Na}_2\text{O}:\text{Al}_2\text{O}_3:2\text{SiO}_2:100\text{--}200\text{H}_2\text{O}$ at $70\text{ }^\circ\text{C}$ (Xu et al., 2007).

2.6.4 Effect of temperature

The researchers are also interested in studying the synthesis temperature to investigate the crystal growth, solid yield and morphological properties of zeolites (Auerbach et al., 2003). The variation effect of temperature is significant because it affects the polymerization reaction between aluminate and polysilicate species by increasing the speed of the polymerization rate with increasing the temperature (Xu et al., 2007). In addition, with an increase in the temperature, the rate of crystal growth increases but the nucleation and induction time decrease (Khajavi et al., 2010). As a result, at high temperature, zeolites can be obtained at shorter time. Moreover, the size of the crystals also increases when the temperature is increased. Furthermore, high temperature also tends to crystallize zeolites with smaller and less opening pores which zeolites with more opening and larger pores are normally crystallized under low temperature. The heating temperature also affects the zeolite phase transformation. Figure 2.8 illustrates the effect of temperatures on the LTA-type zeolite. Here, the

structures of zeolite are recrystallized and transformed into other denser crystalline phase which are more thermodynamic and kinetic stable (Maldonado et al., 2013).

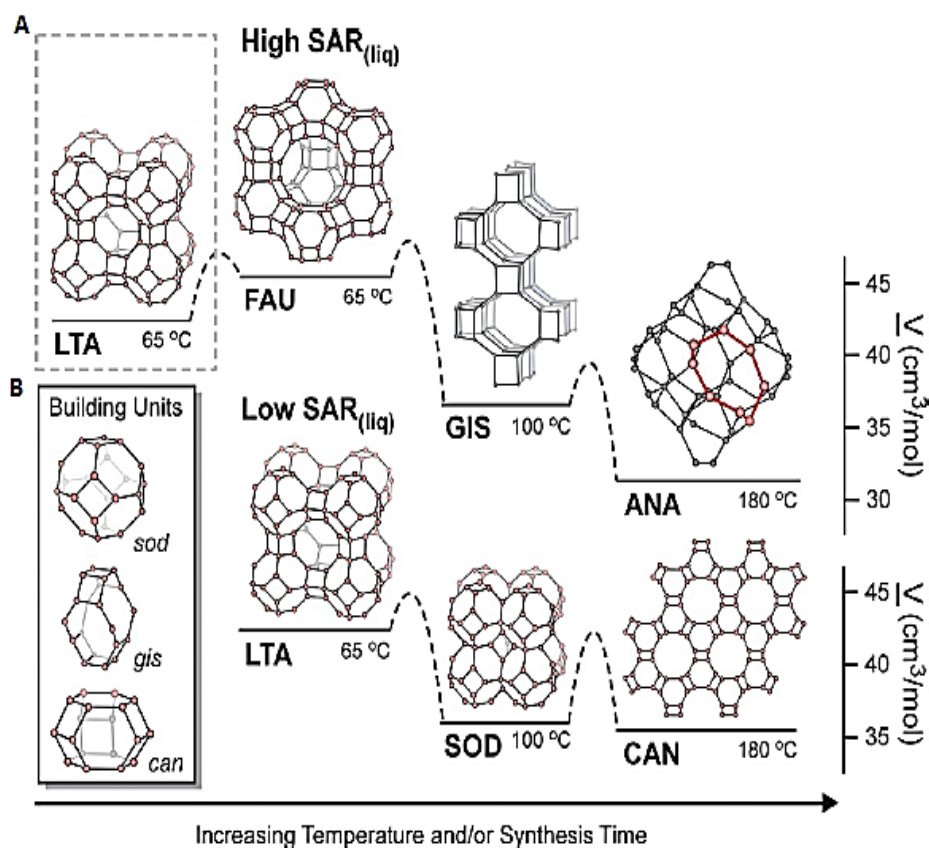


Figure 2.8. Phase transformation of Na-zeolites under increasing hydrothermal heating time and/or temperature (Maldonado et al., 2013).

2.6.5 Effect of time

The crystallization time has great influences on the purity and quality of zeolite produced. Also, there is a strong relationship between the synthesis temperature and the heating time. For example, the zeolite synthesis at low temperature needs a longer time to form zeolite crystals and vice versa (Johnson and Arshad, 2014). Ogura et al. prepared FAU-type zeolite at 90 °C for 24 h (Ogura et al., 2003). They observed other zeolite phases such as chabazite (CHA), sodalite (SOD), and analcime (ANA) were also formed when the synthesis time is further extended to 48 h. Similarly, Ng et al.

prepared the EMT-type zeolite at very low temperature (30 °C) for 36 h, and with prolonged synthesis time it led to the formation of SOD-type zeolite (Ng et al., 2012)

2.6.6 Effect of mineralizing agents (OH⁻ and F⁻)

The concentration of hydroxide (OH⁻) plays an important role in the entire synthesis process of zeolites including crystallization rate, crystal size, the Si/Al ratio of the zeolite formed, and the type of zeolite produced. When increasing the concentration of OH⁻, an increase in the solubility of silica and aluminum is expected where high solubility of the inorganic sources increases the level of supersaturation of the solution which further increases the rates of nucleation and crystal growth within a short time (Feng et al., 2016). When increasing the concentration of OH⁻, some additional phases of zeolite may be formed. Thus, the calculation for the use of optimum amount of OH⁻ is important where the amount of OH⁻ is contributed by many sources such as the silica, alumina, organic template and any additional alkali or alkali earth metal hydroxides (Cejk et al., 2017).

Besides OH⁻, another type of mineralizing agent used in the zeolite synthesis is fluoride (F⁻) ion. The F⁻ anion has been known as a very effective mineralizer in the synthesis of silica-rich zeolites and in the synthesis of zeolites with large crystal sizes (Yu, 2007). In addition, by using F⁻ route, the zeolite synthesis can be performed in acidic to neutral media because it does not affect on the pH value like OH⁻. However, the F⁻ effects in the solubility of inorganic reactants and supersaturation are much lower than OH⁻. As a result, the synthesis of zeolite by using F⁻ media usually requires high temperature and long reaction time (Sanhoob & Muraza, 2016).

2.6.7 Effects of water content

Basically, water is used as a solvent in the hydrothermal synthesis of zeolites (Li & Liu, 2010). The amount of water affects the concentration of reactant in the hydrogel solution, and further impacts the crystal size and the yield of solid product. At low amount of water, it increases the supersaturation condition of mother liquor which affects the nucleation step and produces the crystal particles with small sizes. For example, Sashkina et al. studied the effect of $\text{H}_2\text{O}/\text{SiO}_2$ ratio in the synthesis ZSM-5 zeolite (Sashkina et al., 2017). The crystal size decreased from 1250 to 180 nm with decreasing the H_2O content in the hydrogel solution ($\text{H}_2\text{O}/\text{SiO}_2$ ratio decreased from 10 to 300). In addition, the water content also affects the type of zeolite framework formed (Sashkina et al., 2017). Miyamoto et al. explained the effect of $\text{H}_2\text{O}/\text{SiO}_2$ ratio (2.3 to 45) on the synthesis of CHA-type zeolite (Miyamoto et al., 2015). Pure CHA-type zeolite was obtained with a ratio of 3.8 to 5.3. At the ratios of 2.3, 6.0 and 6.9, the solid product with mixed crystals of CHA and STT phases was obtained. But, when the ratio was increased to the range of 9.8 to 23, pure STT-type zeolite was produced. Another interesting observation was that no XRD signal was observed at high $\text{H}_2\text{O}/\text{SiO}_2$ ratio (>23) and only a broad band was shown, indicating the existence of an amorphous phase (Miyamoto et al., 2015).

The importance of water content in the hydrogels has been reviewed and summarized in Figure 2.9 (Oleksiak and Rimer, 2014). It is found that the ideal water content, z (in the molar ratios of $10 \text{ OH}^- : z \text{ H}_2\text{O}$), to obtain zeolite phases is in the range of 50-1000 where $100 < z \leq 200$ is the most ideal water amount used for the synthesis of zeolites. In this range of water content, 21 different framework structures have been crystallized and 293 publications have been reported (Oleksiak & Rimer, 2014).